RedFame

Studies in Engineering and Technology
Vol. 5, No. 1; August 2018
ISSN 2330-2038 E-ISSN 2330-2046
Published by Redfame Publishing
URL: http://set.redfame.com

# Optimization of the $HgI_2$ Crystal Preparation for Application as a Radiation Semiconductor Detector

João F. Trencher Martins[1], Robinson A. dos Santos[1], Cauê de M. Ferraz[1], Rene R. Oliveira[1], Michael Fiederle[2], Rafael de A. Amadeu[1], Rodrigo S. dos Santos[1], Thiago L. B. da Silva[1], Margarida M. Hamada[1]

[1]Institute for Energetic and Nuclear Research - IPEN/CNEN - SP, São Paulo, Brazil

[2]Freiburg Materials Research Center - University of Freiburg, Freiburg, Germany

Correspondence: Margarida Mizue Hamada, Instituto de Pesquisas Energéticas e Nucleares – IPEN/CNEN-SP, Av. Prof. Lineu Prestes, 2242, 05508-000 São Paulo, Brazil.

Received: July 16, 2017 Accepted: March 26, 2018 Online Published: March 31, 2018

doi:10.11114/set.v5i1.3149 URL: https://doi.org/10.11114/set.v5i1.3149

## Abstract

The effect of $HgI_2$ crystal encapsulation using different polymer resins, with the intent of avoiding the oxidation of the crystal surface, was evaluated in this work. The crystal was purified and grown by the physical vapor transport (PVT) technique modified. Systematic measurements were carried out for evaluating the stoichiometry, structure orientation, surface morphology and impurity of the crystal grown. The purer region of the crystal grown was selected to be prepared as a radiation detector, applying water-based conductive ink contacts and copper wire on the crystal surfaces. After that, the crystal was encapsulated with a polymeric resin which insulates atmospheric gases, aiming to improve the stability of the $HgI_2$ detector. Four resins were used for crystal encapslation and the performance of the detector depended on the composition of the resins used. Among the four resins studied to evaluate the influence of encapsulation on the performance of crystals, as a radiation detector, the best result of resistivity and energy spectrum was obtained for the resin #3 (50% - 100% of Methylacetate and 5% - 10% of n-butylacetate). The encapsulation of crystals with polymer resins, performed with the intent of avoiding the oxidation of the crystal surface, did not compromise the measurements and were fully capable of detecting the presence of gamma radiation. The stability of the encapsulated HgI2 crystal detector was of up to 78 hs, while the stability found for $HgI_2$ detector no encapsulated was in order 3 ~4 hs.

**Keywords:** semiconductor crystal, radiation detector, mercury iodide crystal, surface morphology

## 1. Introduction

$HgI_2$ is a layered semiconductor material with a wide band gap energy (Eg = 2.13 eV), high resistivity ($>10^{14}$ Ωcm), high density (7.5 g/cm$^3$) and high atomic number elements ($Z_{Hg}$=80 and $Z_I$=53. These characteristics make the mercury iodide ($HgI_2$) a very promising material, with large technological applicability as a room temperature radiation detector (Squilante et al., 1995, Goorsky et al, 1996 Gregor & Hermon, 1997). However, problems still exist to grow $HgI_2$ crystals with suitable purity and surface morphology to be used as a room temperature radiation detector. A technological challenge remains (Martins et al, 2012, Zhaojun, et al., 2015, Rault et al, 2016, Barthaburu et al., 2016, Tyagi, 2017).

Most of semiconductor crystals, such as $PbI_2$ (405°C) (Oliveira, et al, 2002), TlBr (468°C) (Oliveira et al, 2004, Santos et al, 2017 and $BiI_3$ (408.6°C) (Ferraz et al., 2017) are purified and grown by the fusion technique However, the $HgI_2$ undergoes structural phase transition below its melting point (259°C), what makes its growth by fusion technique more difficult (Zhou et al.. 2003; Martins et al. 2012). $HgI_2$ can present three solid phases, being differentiated by structural features. One of the phases is known as α-$HgI_2$, of red color, and it is obtained below the transition temperature, around 127°C. Its structure is tetragonal and is the most stable of all phases of $HgI_2$ (Ariesanti et al., 2010,). Another phase is the β-$HgI_2$ of yellow color with orthorhombic structure and it can be obtained in different ways, generating two different types of characteristic polymorphisms. One way of obtaining it is above the transition temperature, i.e. above 127° C, this is known as yellow$^{HT}$ (HT - High Temperature) and it is in a complete $HgI_2$ transition phase, but not totally stable. Another form is metastable, known as yellow $^{M}$ (M - metastable), and it is obtained by a rapid evaporation of a solvent, which can be below the transition temperature. The third phase of this material is known as orange $HgI_2$, only having differences in the positions of the mercury atoms between the atoms of iodine. Thus, the fusion technique is not recommended for the growth of $HgI_2$, other techniques, such as "Physical Vapor Transport" (PVT) (Zhou et al, 2003) or “Saturated Solution” (Rao et al, 1979) are more adequated for $HgI_2$ growth.

The performance of radiation semiconductor detectors is controlled by both intrinsic and extrinsic factors. Carrier lifetime, mobility and the atomic number of the material used for radiation detectors represent intrinsic parameters, while extrinsic factors such as crystallographic perfection, surface morphology and stoichiometry and impurity levels can also play a major role in the performance of radiation detectors (Goorsky et al, 1996, Oliveira 2004).

The impurities can influence the charge carrier lifetime and the surface morphology, affecting the detector efficiency. There is agreement in the literature on the difficulty in growing crystals with high crystallographic perfection, high chemical purity and good stoichiometry and surface morphology, suitable to be used as room temperature semiconductor detectors [Oliveira et al., 2004, Ariesanti et al, 2010, Marcondes et al, 2011, Santos et al., 2017). The role of the crystal impurities on the electrical properties and surface morphology of $HgI_2$ is crucial, and the performance of these detectors has been limited by the crystals quality.

Studies have been carried out to establish a correlation between the roughness and surface morphology with the resulting values of the detector leakage currents. It has been demonstrated that using smoother surfaces, lower noise is produced in the detectors [Squilante et al. 1995, Oliveira et al. 2005, Martins et al., 2012). However, as far as we know, studies related to the influence of crystal encapsulation on its performance as a radiation detector has not been, previously, reported. In this work, the radiation response was studied encapsulating the $HgI_2$ crystal detectors with polymer resins of different compositions. The encapsulation was carried out immediately after the preparation of the crystal as a radiation detector, applying electrical contacts on the crystal surfaces. It was demonstrated, at first time, the influence of the encapsulation in radiation detector performance. Also, improvements in the purification and growth of the HgI2 crystal were accomplished and its quality evaluated.

## 2. Method

The commercially available $HgI_2$ powder (Alpha Aesar), with nominal purity of 99.9%, was used as the starting material for growing crystals. The crystals were purified and grown by PVT technique. For purification of the $HgI_2$ powder, the PVT method was modified, whose scheme is shown in Figure 1. The heat is provided by a resistive wire which covers the bottom of the tube (Figure. 1E), heat exchange (Figure 1B) is performed by flowing water (Figure. 1A). The system is wrapped in a metal housing to reduce heat loss to the environment.

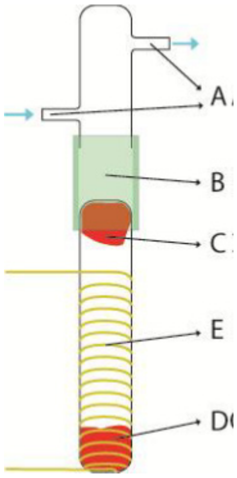

Figure 1. Scheme of the $HgI_2$ powder purification system: (A) cooler water flow, (B) heat exchange region (C) purified $HgI_2$, (D) $HgI_2$ powder and (E) resistive wire

For purification, the borosilicate glass ampoule filled with 5 g of $HgI_2$ powder was, previously, evacuated at 90°C for 15 min and sealed, aiming the powder dehumidification and prevention of $HgI_2$ vapor loss, with external contamination. Afterward, the ampoule containing $HgI_2$ powder, at the bottom (Figure 1D), is placed in the purification system. The $HgI_2$ powder heated at 110°C sublimes in the upper region of the ampoule (Figure 1C), being deposited in the heat exchange region. The residue of the raw material remained at the ampoule bottom. This purification process is based on sublimation difference among the $HgI_2$ and powder contaminants, thus, when $HgI_2$ is heated, it converts into the vapor phase; contaminants with different sublimation temperatures are separated from $HgI_2$.

The $HgI_2$ crystal growth was, also, performed by PVT technique. Growth theory is quite similar to the purification, differing only by the parameters of temperature and time, as well as the furnace and ampoule used.

The heat is transmitted from a sealed resistance contained within the furnace (Figure 2), which has outer stainless steel walls in order to reduce the loss of heat to the environment and provide structural resistance, as can be observed on the furnace schema (Figure 3). For growth, the ampoule containing the purified solid $HgI_2$ should be hermetic in order to prevent loss of $HgI_2$ vapor and reduce the possibility of contamination or loss of stoichiometry in the grown crystals.

The time and temperature parameters were found by equation (1) where the Qmax value is the quantity of the purified solid $HgI_2$ placed in the ampoule, T is the temperature in the hottest region of the furnace and k is proportionality constant.

The impurity concentration, surface morphology and stoichiometry of the $HgI_2$ crystal were analyzed by the scanning electron microscopy with back-scattered electrons (SEM-BSE) technique, using the scanning electron microscopy (SEM-BSE), LX 30 Philips model. The acceleration voltage used for measurements was 20kV.

$$\frac{dT}{dQ} = e^{-kQ}(Q_{max} - Q) \tag{1}$$

(A) (B)

Figure 2. Furnace designed for $HgI_2$ crystals growth (A). Growth ampoule containing the $HgI_2$ crystal grown on the top and growth residues on the bottom of the ampoule

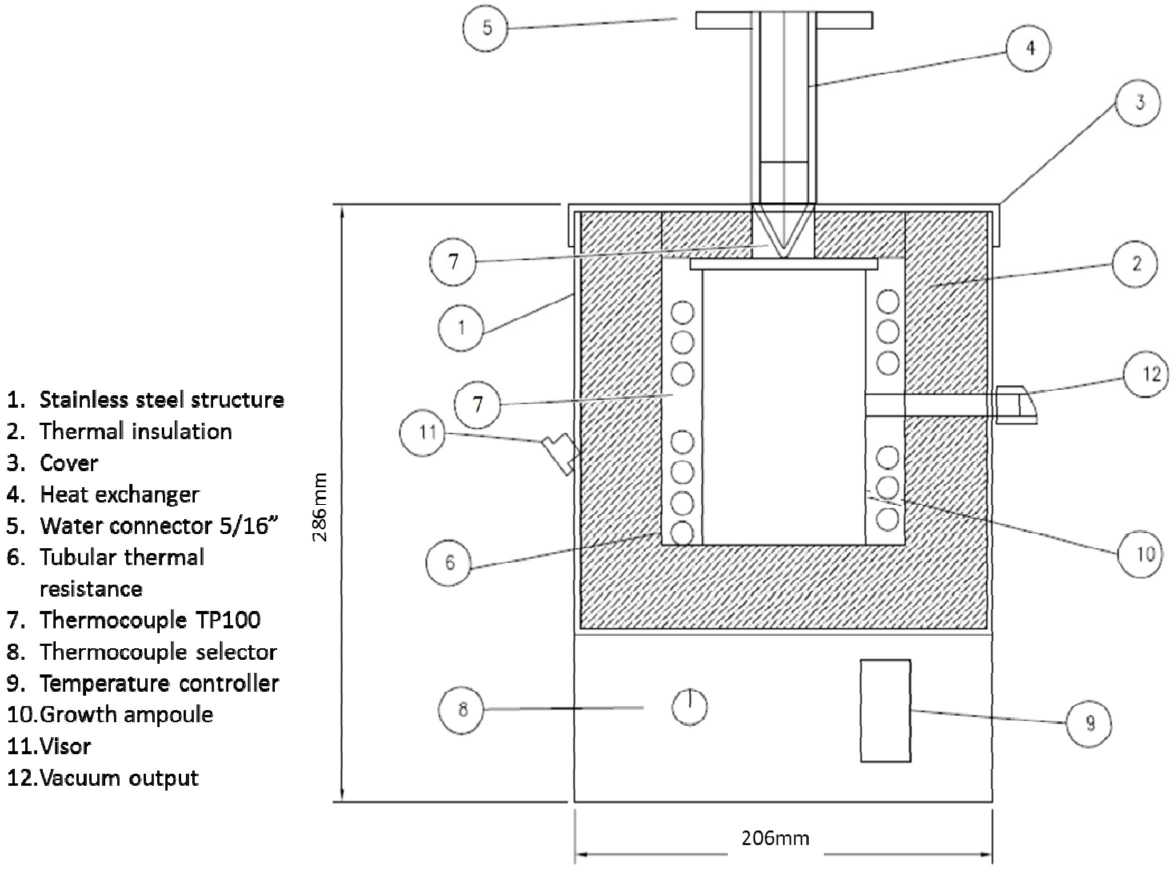

Figure 3. Furnace schema

The crystalline quality and structural characterization of the $HgI_2$ crystal were analyzed by X-ray diffraction (XRD). X-ray diffraction patterns were obtained in a Siemens (D5005) Diffactrometer, using CuKα radiation (2θ ranging from 10° to 100º). The samples were measured with a scan rate at 2 °/ min and the step size of the X-ray diffraction analysis was of λ = 1,5418Å.

After the physicochemical characterizations, crystals with better characteristics were selected to be prepared as radiation detector. Firstly, the crystal was cleaved using a thin ceramic blade at low pressure along its axis to cleaving the crystals. $HgI_2$ is highly reactive with metals, thus the use this material should be avoided, being the ceramic more suitable. Applying a force or knock, minerals may break with certain particularities, often reflecting the crystal structure. The $HgI_2$ crystal has a cleavage plane along its axis <100>, due to lower bond energy between atoms and greater interatomic spacing. Among iodine atoms there is 151kJ/mol of bond energy and between iodine atoms and mercury atoms that energy is 291kJ/mol, this lower energy is resulting interactions enters atoms less intense, leading to greater crosslink spacing, this can best be understood in Figure 4.

The final dimensions of the crystal slices were approximately 10 mm diameter and 1 mm thick. Studies for the preparation of $HgI_2$ crystals as radiation detectors were carried out at the Materials Research Center (FMF-Freiburger Materialforschungszentrum) of the Universität Freiburg. The $HgI_2$ radiation detectors were prepared, placing electrical contacts on the cleaved slices of the $HgI_2$ crystal, to make it possible to measure the charge carriers produced under the ionizing radiation excitation. The conductive graphite ink (Viatronix) and copper wire contacts were applied on opposite sides of the newly cleaved crystals, as quickly as possible, in order to minimize the reactions between the exposed crystal surfaces and the atmosphere. After about two minutes (required to dry the conductive paint) the crystals were coated with polymer resin in order to isolate the atmosphere and evaluate the performance of the detector after resin encapsulation as to its response to radiation.

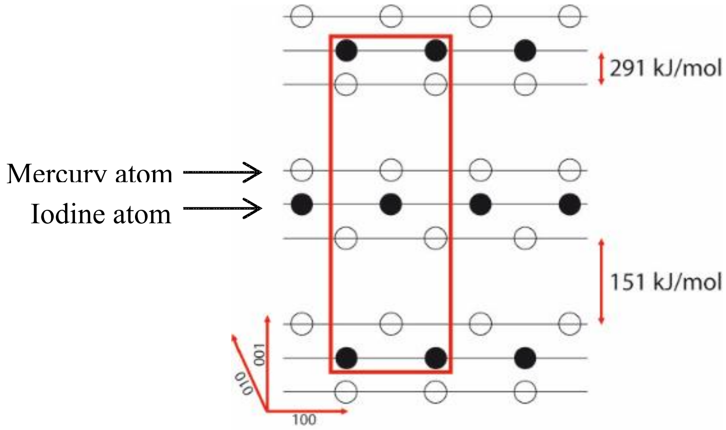

Figure 4. Crystalline planes of tetragonal $HgI_2$ crystal

Four types of commercial polymer resins were used to evaluate the influence of the resin type on the performance of the crystals, as a radiation detector. The compositions of the commercial resins used are summarized in Table 1.

Table 1. Composition of resins

| | | | |
|---|---|---|---|
| Resin #1: | 50% - 100% Heptane ($C_7H_{16}$)<br>10% - 25% Methylcyclohexane ($C_6H_{11}CH_3$)<br>< 1% Cyclohexane ($C_6H_{12}$) | Resin #3: | 50%- 100% Methylacetate ($CH_3COOCH_3$)<br>5% - 10% n-butylacetate ($CH_3COO(CH_2)_3CH_3$) |
| Resin #2: | 25% - 50% ethanol ($CH_3CH_2OH$)<br>25% - 50% acetone ($CH_3COCH_3$)<br>< 2,5% ethyl acetate ($CH_3COOC_2H_5$) | Resin #4: | 50% -100% ethyl-2-cyanoacrylate ($C_6H_7NO_2$) |

The sequence of the preparation steps of the crystal of $HgI_2$ as a detector of radiation after the growth and physicochemical characterization, is shown in the Figure 5, that are: (1) crystal selection; (2) cleavage of crystal; (3) electrical contact application to collect the electrical signal and (4) crystal encapsulation with the resin, in order to inhibit to oxidation and reduce the current generated in the crystal surface and (5) electronic coupling.

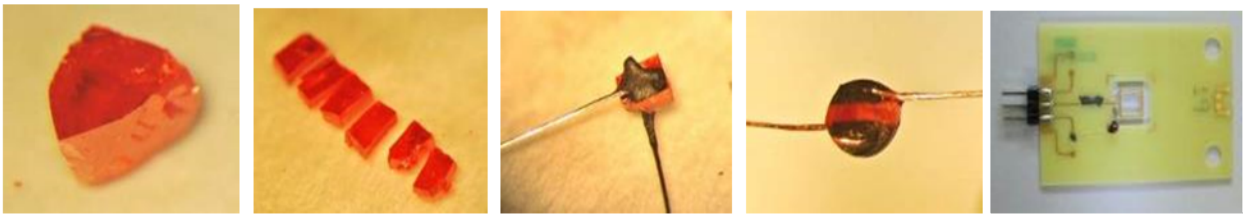

(a) (b) (c) (d) (e)

Figure 5. Preparation sequence of the HgI2 crystal detector: (a) Crystal grown, (b) crystal cleaved, (c) Crystal surface with contact applied, (d) Crystal detector encapsulated with resin and (e) Crystal detector coupled to the electronics

In order to evaluate the leakage currents and resistivity of the detectors developed in this work, leakage currents were measured by applying a potential over the semiconductor using an adjustable voltage source, Ortec model 556 and the current value was obtained using an ammeter, Model 619, Keithey. In order to avoid mechanical shocks and incidence of light, the crystal detector was packed in an aluminum box.

With the values obtained from the measurements, the resistivity of the detectors was determined, by inference to the leakage current values, using the following equation (2):

$$\rho = \frac{V\ A}{I_d\ l} \tag{2}$$

where, ρ is the resistivity in the dark, V is the voltage applied in volts, The contact area is $cm_2$, $I_d$ is the current in the dark given in Ampére and l is the sample thickness in cm [Knoll, 1989].

For the measurements of the radiation, the encapsulated detector was packed in an aluminum housing, which acts as an electromagnetic and optical shield and then coupled to the preamplifier. Energy spectra were measured using a $^{137}Cs$ gamma radiation source (662 keV) and a conventional oscilloscope (Tektronix MSO5104B 1Ghz). Measurements were performed at room temperature (24°C).

## 3. Results and Discussion

A brilliant dark red color crystal with 15 mm maximum diameter and 20 mm thickness, obtained by PVT method and a crystal wafer, after cleavage, with a deep red color, are shown in Figures 6 (a) and (b), respectively. Crystals of 1 $cm^2$ superficial area and 0.5 cm thickness, with regular angulations plus uniform and transparent surface were obtained, as it may be observed in these figures.

$HgI_2$ grown by PVT (a) Crystal cleaved by PVT (b)

Figure 6. Crystal original form re-grown by PVT (a) after the cleavage (b) magnified 50X with optical microscopy

The typical X-ray diffraction pattern of the cleavage surface from $HgI_2$ crystals grown is shown in Figure 7. The results showed that the crystals have a similar structure to the tetragonal crystalline pattern of the $HgI_2$. The X-ray diffraction pattern indicates that the crystal is, preferentially, oriented in the (001) and (101) directions. Similar result was found by Ariesanti et al [2010 b].

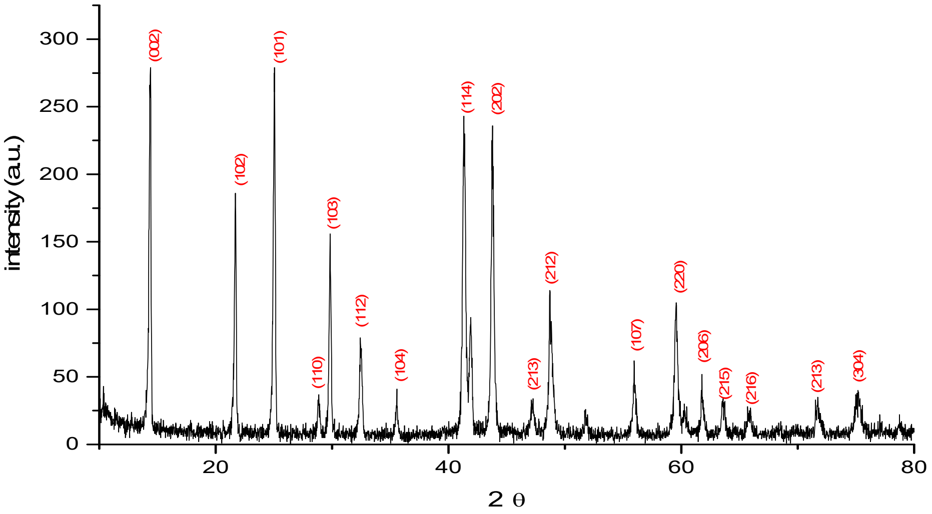

Figure 7. X-ray diffraction pattern of $HgI_2$ grown by PVT

The $HgI_2$ crystal grown by the PVT technique, which is at the top of the ampoule, is shown in Figure 8 (a), while its elemental composition and stoichiometry determined by the SEM-BSE method are shown in Table 2. Three samples were extracted at different regions of the crystal surface, aiming to verify the uniformity of whole surface of the crystal. As can be seen in the Table 2, adequate stoichiometry was found in all three samples, confirming uniformity in all crystal regions. For example, for sample 1 the atomic percentage of Hg was 28.53, while for $I_2$ it was 55.52, corroborating a good stoichiometry for the $HgI_2$ crystal. Also, the samples 2 and 3 presented close results. Other elements, such as Al, Si, K, were observed in the trace form, acting as impurities in the crystal. The atomic percentage around 14% found in $O_2$ can be attributed to the surface exposure of $HgI_2$ in atmospheric air. It should be noted that adequated stoichiometry was found at the three regions extracted of the crystals, indicating the homogeneity on the whole surface of the crystals These results demonstrate the efficiency of PVT as a purification method and SEM-BSE to determine the concentration of impurities and stoichiometry.

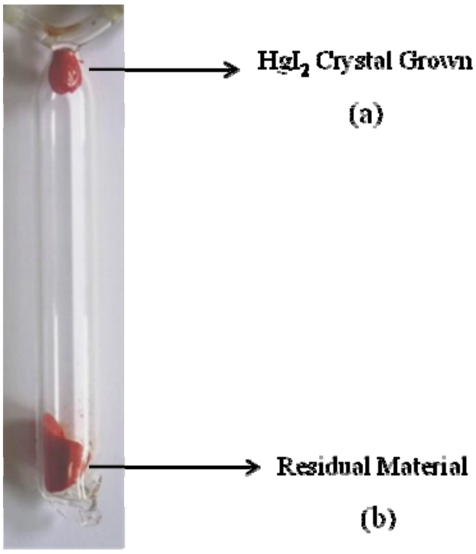

Figure 8. Picture of $HgI_2$ crystal inside its growth ampoule

Table 2. Elemental composition of the $HgI_2$ crystal surface grown by PVT technique

| | **Sample 1** | |
|---|---|---|
| Element | % atomic | Error % |
| O | 13,59 | 11,90 |
| Al | 0,47 | 141,02 |
| Si | 1,20 | 48,97 |
| **Hg** | **28,40** | **1,63** |
| K | 0,64 | 58,85 |
| **I** | **55,70** | **1,59** |
| | **Sample 2** | |
| Element | % atomic | Error % |
| O | 13,99 | 11,10 |
| Al | 0,00 | 0,00 |
| Si | 1,29 | 46,99 |
| **Hg** | **28,53** | **1,65** |
| K | 0,86 | 42,04 |
| **I** | **55,52** | **1,57** |
| | **Sample 3** | |
| Element | % atomic | Error % |
| O | 14,34 | 8,75 |
| Al | 0,00 | 0,00 |
| Si | 1,32 | 40,60 |
| **Hg** | **28,17** | **1,53** |
| K | 1,27 | 25,91 |
| **I** | **54,91** | **1,53** |

Figure 9 shows the micrographs of the scanning electronic microscopy with secondary electrons (MEV-SE) carried out in the cleaved slice from the $Hg_2$ crystal grown by the PVT technique, in order to evaluate the quality of the $HgI_2$ surface. As can be seen in this Figure, the crystal magnified 200 times presented smooth surface (Figure 9a). Extending 650 times a structure with uniform layers can be observed (Figure 9b), indicating a good orientation in the crystal structure.

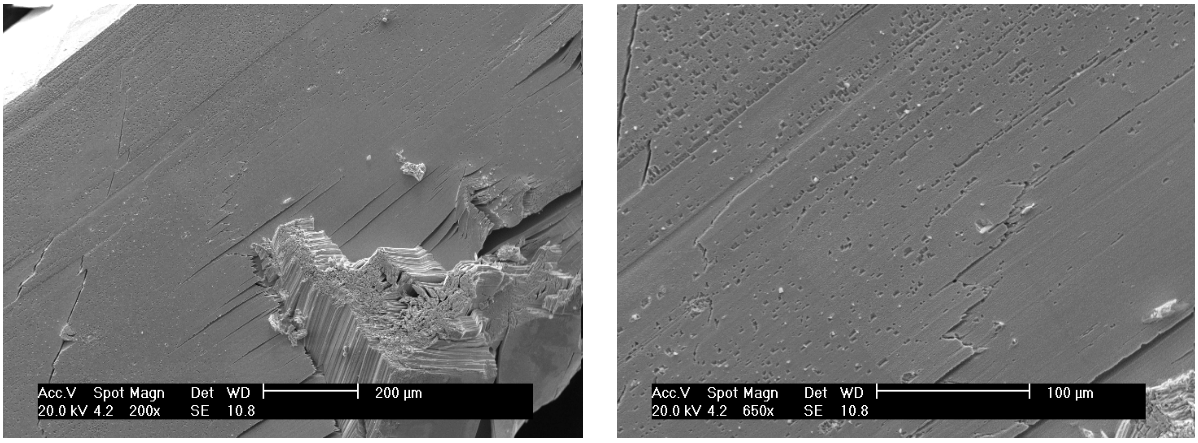

Expanded 200X (a) Expanded 650X (b)

Figure 9. MEV-SE micrographs of the $HgI_2$ crystal surface grown by PVT

In addition, the micrographs of the scanning electron microscopy with back-scattered electrons (SEM-BSE) carried out in the slice leaved from the $HgI_2$ crystals grown by PVT is showed in Figure 10. A structure with uniform layers may be also observed, even magnifying the image 5000 times (Figure 9), confirming a good orientation in structure of this crystal.

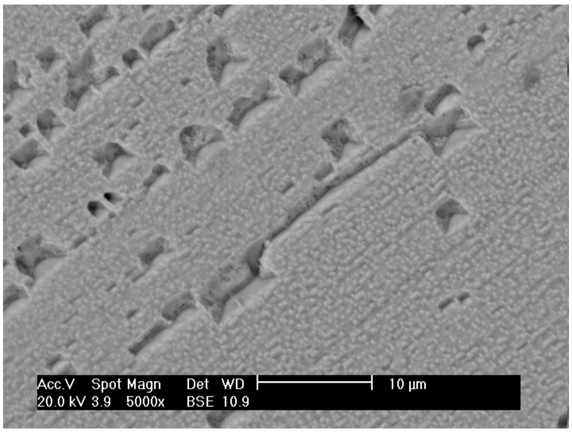

Figure 10. SEM-BSE micrographs of the $HgI_2$ crystal surface grown by PVT (expanded 5000X).

The residue of the raw material remained at the ampoule bottom after the crystal growth by the PVT (Figure 8(b)) was, also, evaluated by the SEM-BSE technique. The results summarized in the Table 3 were compared with those obtained for the $HgI_2$ crystal grown at the top of the ampoule (Table 2). The presence of significant amounts of impurities can be observed, namely, O, Na, Mg, Al, Si, K, mainly potassium, K, (21.41% ) and oxygen, O, (53.28%), which were higher than those of Hg (4.35%) and I (4.54%). The stoichiometry of $HgI_2$ was not followed in this sample, contrary to that found in the $HgI_2$ crystal grown. This result confirms the efficacy of the PVT technique to purify the starting material and SEM-BSE to determine the impurity concentration.

Table 3. Elemental composition from the $HgI_2$ residual salt after the crystal growth by PVT method.

| Element | % atomic | Error (%) |
|---|---|---|
| O | 53.28 | 16.61 |
| Na | 3.27 | 1.44 |
| Mg | 2.84 | 1.52 |
| Al | 6.84 | 3.84 |
| Si | 3.47 | 2.02 |
| Hg | 4.35 | 6.54 |
| K | 21.41 | 19.99 |
| I | 4,54 | 3,65 |

Figure 11 shows the residual powder surface layer from the bottom ampoule after the growth obtained by SEM-BSE technique. As it can be seen from this Figure, the image showed an amorphous structure, as expected, since the crystal must be formed at the upper extremity of the ampoule.

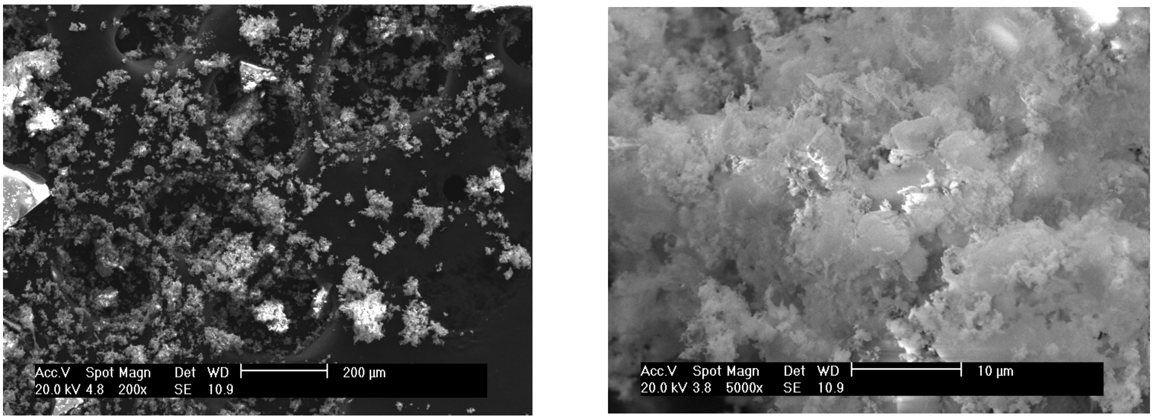

(a) (b)

Figure 11. SEM-BSE micrographs of the $HgI_2$ residual powder remained at the bottom of the ampoule after the growth, expanded 200 X (a) and 5000 X (b)

The purer region of the crystal grown by PVT technique was selected to be prepared as a radiation detector, applying water-based conductive ink contacts and copper wire on the crystal surfaces. The deposition of contacts in any device merits significant attention and, in the case of $HgI_2$, this attention should be even greater since the $HgI_2$ is extremely reactive with a large range of metals, thus the contacts should be carried out with non-conductive materials, such as conductive inks containing carbon particles. Some authors (Perez et al. (2009), Schieber et al(2001) point out, as an alternative, the contacts with two carbon material particles, palladium and rhodium, however up to the present moment it is agreed in the literature (Coleman (1978), Kaldis (2008)) that the contacts with conductive inks are better for use with $HgI_2$. Thus, the use of water-based conductive paint has overcome a major drawback, which is the high reactivity between metal contacts and the surface of $HgI_2$ crystals.

After, approximately, two minutes (necessary for drying the conductive ink), the crystals were coated with a polymeric resin which insulates atmospheric gases, aiming at minimizing the reactions between the exposed surfaces and these gases. Among the four resins studied (Table 1) to evaluate the influence of encapsulation on the performance of crystals, as a radiation detector, a chemical reaction between the crystal surface coated with resin #1 (50%-100% Heptane; 10%-25% Methylcyclohexane and <1% Cyclohexane) and the copper conductive wire components was observed during the polymerization process, what may be associated to the formation of free radicals. This reaction may be observed within a few minutes after the polymerization, with the formation of bubbles and alteration of the resin color, as shown in Figure 12a. In comparison, there are no evidences of chemical reactions during the polymerization of resin #3 (methyl-acetate e n-butyl-acetate), as well as of resin number 2 (ethanol, acetone e ethyl-acetate) and 4 (ethyl-2-cianoacrilate), as it may be seen in Figure 12b.

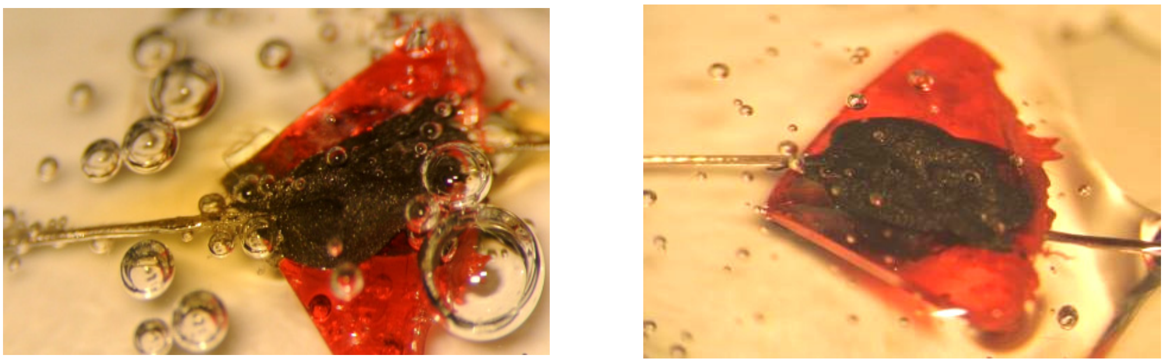

(a) (b)

Figure 12. Detector encapsulated with resin #1 (a) and Detector encapsulated with resin #3 (b)

After preparation of the $HgI_2$ crystal as a radiation detector, its performance on the radiation response was evaluated. At first, resistivity values of the $HgI_2$ crystals were determined by the leakage current measurements as a function of the applied voltage. The determined resistivity values from each crystal encapsulated are summarized in Table 4. The best resistivity result (3.9 x 1010 Ωcm) was obtained for the detector encapsulated with resin #3 (50% - 100% of methyl-acetate and 5% - 10% of n-butyl-acetate), which value is close to those described by Zhang et al (2015). It was not possible to evaluate the crystal encapsulated with resin # 1 due to the chemical reaction occurrence between the resin and the $HgI_2$ crystal surface with the electric contacts (Figure 12a), not allowing its use as a radiation detector.

Table 4. Resistivity values of the $HgI_2$ crystal encapsulated with different polymeric resins.

| | **Resistividade (Ωcm)** |
|---|---|
| Resin # 1 | **ND** |
| Resin # 2 | $8.5 \times 10^7$ |
| Resin # 3 | $6.4 \times 10^8$ |
| Resin # 4 | $3.9 \times 10^{10}$ |

As far as it is known, all works found in the literature aiming at studying the effect of stability of $HgI_2$ detectors are focused either on the study of purity and defects of crystals, or the morphologic quality of their surfaces. For the first time, the encapsulation of the $HgI_2$ crystal has been proposed in order to avoid the oxidation of the surface with the intent of avoiding the oxidation of the crystal surface, thus increasing the stability of the $HgI_2$ detector.

Figure 13 shows the 662 keV energy spectra from the $^{137}Cs$ source of fifteen $HgI_2$ detectors, divided into three batches of samples from three different crystals. Each batch was prepared using $HgI_2$ crystals of the same origin, which were encapsulated with four different resins. In this study, it was observed that the detector performance depends on the resin composition. As it may be seen in the three spectra of Figure 13, the resin that presented the best performance was resin #3, which is composed of 50% - 100% of methyl-acetate and 5% - 10% of n-butyl-acetate. All crystals encapsulated with resin #3 presented better spectrometric results (Figure 13), with photopeak more clearly observed.

The spectra from crystals encapsulated with resins 2 and 4, although sensitive to radiation, did not present energetic resolution to form the photopeak. A possible explanation may be the formation of ionic free radicals that can conduct electric current; however, more detailed studies should be carried out. The crystal encapsulated with resin#1 was not measured, because its reaction with the electric contacts (Figure 12a), disables its use as a radiation detector.

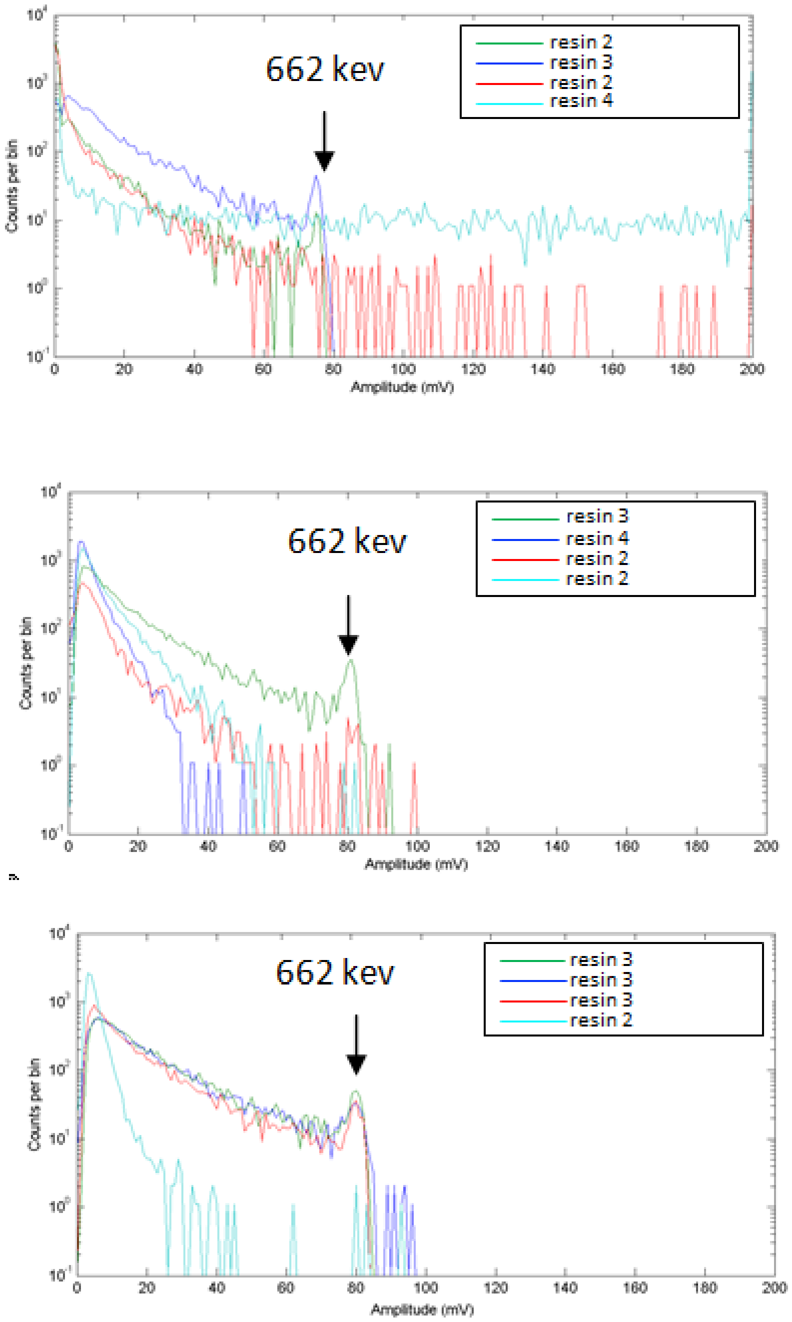

Figure 13. Energy Spectrometry obtained for different encapsulation resins used

The stability was evaluated by the degradation of the photopeak from the spectra in function of the time. The stability found in $HgI_2$ crystals without the encapsulation were around 3~4 hours, while for detectors encapsulated with resin #3 (Table 1) in this work the stability lasted till 78 hours.

## 4. Conclusion

$HgI_2$ crystals grown by the PVT method presented a high purity, good morphology surface quality and orientation in the crystal structure, showing to be suitable for the use as a room temperature radiation semiconductor detector. The dependence of the detector performance on the resin composition used in the crystal encapsulation was demonstrated in this work. Among the four resins evaluated, the best performance was found for resin #3, whose composition is 50% - 100% methyl acetate and 5% to 10% n-butyl acetate. The crystal encapsulated with this resin presented a well-defined photopeak in its energy spectrum, as well as, the best resistivity value of the order of 3.9 x $10^{10}$ Ωcm . The other two resins studied, resine #2 (25% - 50% ethanol, 25% - 50% acetone and <2.5% ethyl acetate) and resine#4 (50% -100% ethyl-2-cyanacrylate) were sensitive to radiation, however, no photopeak was observed. The resistivity value found for the HgI2 detector encapsulated with resin #2 was 6.4 x $10^8$ Ωcm and resin # 4 was of 8.5 x $10^7$ Ωcm. A chemical reaction between the resin# 1 (50% - 100% Heptane 10% 25% Methylcyclohexane; and 1% Cyclohexane) and electrical contacts applied to the surface of the crystals was observed, in the resin polymerization for crystal encapsulation, making resin #1 unsuitable for its use in the preparation of the crystal as a radiation detector. The stability of the $HgI_2$ detectors without the encapsulation was in the order of 3 to 4 hours, while the detectors encapsulated in this work presented stability of up to 78 hours, corroborating the validity of the encapsulation.

## Acknowledgements

The authors express their acknowledgments to Christian Disch for energy spectrometry measurements and to FAPESP-SP (grant: 12/05254-9) and CNPq (grant: 305210/2013-0) for the financial support. The authors C. M Ferraz and J. F. T. Martins thank the CNPq for the fellowship.

## References

Ariesanti, E., Kargar, A., & Mcgregor, D. S. (2010). Fabrication and spectroscopy results of mercuric iodide Frisch collar detectors. Nucl. Instr and Meth. *Phys. Res. A, 624*(1), 656-661. https://doi.org/10.1016/j.nima.2010.09.075

Ariesanti, E., Kargar, A., & Mcgregor, D. S. (2010). Vapor Growth of Tetragonal Prismatic Mercuric Iodide Crystals In: Nuclear Science Symposium Conference Record (NSS/MIC), 2010 IEEE, Knoxville, USA, *1*, 3739-3745. https://doi.org/10.1109/NSSMIC.2010.5874510

Ariesanti, E., Kargar, A., & Mcgregor, D. S. (2010). Vapor Growth of Tetragonal Prismatic Mercuric Iodide Crystals In: Nuclear Science Symposium Conference Record (NSS/MIC), 2010 IEEE, Knoxville, USA, *1*, 3739-3745. https://doi.org/10.1109/NSSMIC.2010.5874510

Barthaburu, M. P., Galain, I., Aguiar, I., Pereira, H. B., & Fornar, L. (2016). $HgI_2$ nanostructures obtained hydrothermally for application in ionizing radiation detection, *J. Phys. D: Appl. Phys., 49*, 445309, 1-6. https://doi.org/10.1016/j.physb.2017.01.013

Ferraz, C. M., Armelin, M. J. A., Oliveira, R. R., Otubo, L., Martins, J. F. T., Santos, R. A., … Hamada, M. M. (2017). Purification and Crystal Growth of the Bismuth (III) Iodide-influence of Trace Impurities on the Crystal Quality, *Studies in Engineering and Technology*, *4*(1), 70-84. https://doi.org/10.11114/set.v4i1.2566

Goorsky, M. S., Yoon, S. M., James, R. B., Mcgregor, D. S., & Natarajan, M. (1996). X-Ray diffuse H. scaterring for evaluation of wide bandgap semiconductor nuclear radiation detectors, *Nucl. Instrum. Meth. Phys. Res. A, 380*, 6-9. https://doi.org/10.1016/S0168-9002(96)00288-4

Knoll, G. (1989). Radiation Detection and Measurement, 2 ed., New York: John Wiley.

Marcondes, R. M., Martins, J. F. T., Santos, R. A., Costa, F. E., Gennari, R. F., & Hamada, M. M. (2011). The Physical Vapor Transport as a technique for purification and growth of the HgI2 crystal. In: International Nuclear Atlantic Conference (INAC/ENAN), INAC2011, Belo Horizonte, Brazil.

Martins, J. F. T., Costa, F. E., Santos, R. A., Mesquita C. H., & Hamada, M. M. (2012). A comparative study on the performance of radiation detectors from the $HgI_2$ crystals grown by different techniques; NUKLEONIKA, *57*(4), 555−562.

McGregor, D. S., & Hermon, H. (1997). Room-temperature compound semiconductor radiation detectors. Nucl. Instr and Meth. Phys. Res. A, *395*, 101-124. https://doi.org/10.1016/S0168-9002(97)00620-7

Oliveira, I. B., Costa, F. E., Armerlin, M. J., & Hamada, M. M. (2002). IEEE Trans. *Nucl. Sci., 49*(4), 1968-1973. https://doi.org/10.1109/TNS.2002.801483

Oliveira, I. B., Costa, F. E., Chubaci, J. F. D., & Hamada, M. (2004). Purification and preparation of TlBr crystals for room temperature radiation detector applications, IEEE. Trans. *Nucl. Sci., 51*, 1224-1228. https://doi.org/10.1109/TNS.2004.829383

Oliveira, I. B., Costa, F. E., Kyohara, P. K., & Hamada, M. M. (2005). Influence of crystalline surface quality on TlBr radiation detector performance, IEEE transactions on nuclear science, IEEE Trans. *Nucl. Sci., 52*(5), 2058-2062. https://doi.org/10.1109/TNS.2005.856788

Pérez, M., Noguero, I., & Fornaro, F. (2009). Properties of electrodes on HgI2 polycrystalline films, Nucl. Instr. and Meth. in Physics Research Section A: Accelerators, Spectrometers, Detectors and Associated Equipment, 328-331. https://doi.org/10.1016/j.nima.2009.05.185

Rao, M. R., & Verma, J. K. D. (1979). Solution grown mercuric iodide crystals as low-energy gamma-ray conduction type detectors. Saha Institute of Nuclear Physics, October 1979.

Rault, M., Binet, L., Gourier, D., Wallez, G., Ponpon, J. P., Biava, D., Inglese, J. M., & Barboux, P. (2016). Textured α-HgI2 ceramics for sensitive X-ray detection Nucl. Instr and Meth. *Phys. Res. A, 808*, 35–40. https://doi.org/10.1016/j.nima.2015.11.032

Santos, R. A., Mesquita, C. H., Silva, J. B. R., Ferraz, C. M., Costa, F. E., Martins, J. F. T., .... Hamada, M. M. (2017). Influence of Impurities on the Radiation Response of the TlBr Semiconductor Crystal, *Advances in Materials Science and Engineering, 2017*, 1-10. https://doi.org/10.1155/2017/1750517

Squillante, M. R., & Shah, K. (1995). Semiconductors for room temperature nuclear detector applications, Semiconductors and Semimetals, *43*. T.E. Schlesinger and R.B. James Ed., Academic Press, 475.

Squillante, M. R., Shah, K., Semiconductors for room temperature nuclear detector applications, (1995). Semiconductors and Semimetals, v.43. T.E. Schlesinger and R.B. James Ed., Academic Press, 475.

Tyagi, P. (2017). Optical band gap demarcation around 2.15 eV depending on preferred orientation growth in red $HgI_2$ films. *Physica B, 510*, 1–6.

Zhang, Z., Zheng, W., Chen, A. Q. A., Ding, K., & Huang, F. (2015). Crystal Growth of α-HgI2 by the Temperature Difference Method for High Sensitivity X-ray Detection. *Cryst. Growth Des., 15*(7), 3383–3387. https://doi.org/10.1021/acs.cgd.5b00468